Multiobjective Optimization of Two-Motor and Two-Speed System for Electric Vehicles Considering Motor Characteristics

Kihan Kwon, *Member, IEEE*, Dong-Min Kim, *Member, IEEE*, Kyoung-Soo Cha, Junhyeong Jo, Myung-Seop Lim, *Senior Member, IEEE*, and Seungjae Min, *Member, IEEE*

***Abstract*— Multimotor and multispeed transmission systems for electric vehicles (EVs) can outperform conventional systems in energy efficiency and dynamic performance. Since motor characteristics directly affect EV efficiency, they were analyzed and verified by the simulation and experiment, respectively. The efficiency and performance of the two-motor and two-speed EV were evaluated using the motor characteristic results, and the importance of the motor design parameters was confirmed to improve them. To maximize both, a multiobjective optimization problem, including the objectives representing electricity consumption per 100 km (EC100) and acceleration time, was formulated. As a solution to the excessive computational burden arising from the optimization process, an artificial neural network (ANN) model was proposed. The ANN-model-based optimization was performed to find the optimal solutions, and a Pareto front, indicating a trade-off between efficiency and performance, was obtained. Furthermore, the results of the optimal motor design values demonstrated the necessity of accurate motor characteristic analysis according to changes in motor design parameters. Finally, the optimization results between various EV powertrain systems were compared to confirm the superiority of two-motor and two-speed systems. Especially, the EC100 and acceleration time were enhanced by up to 11.7% and 14.1%, respectively, compared with a powertrain system employing single-motor and single-speed.**

***Index Terms*— Artificial neural network (ANN)-model-based optimization, electric vehicles (EVs), energy efficiency, motor efficiency characteristic, two-motor and two-speed powertrain.**

I. Introduction

CURRENTLY, the need for reducing anthropogenic gas emissions is widely recognized worldwide. As an alternative to this problem, electric vehicles (EVs) have gained significant attention in various countries [1], and automakers have increased the development of EVs to replace internal combustion engine vehicles (ICEVs) [2]. Because the primary difference between EVs and ICEVs is their respective powertrain system configuration, the powertrain system design should be elaborately performed to satisfy the driving requirements of EVs. In general, the main requirements for a powertrain system design are energy efficiency and dynamic performance. In addition, the key traction components of the powertrain system consist of a motor and a transmission, especially electric motors directly affect the efficiency and performance of the EV [3]; thus, it is essential to design them appropriately to improve the energy efficiency and dynamic performance of EVs.

Three key points for an optimal motor and transmission design for improving the efficiency and performance of EVs are identified from previous studies: 1) system configuration; 2) design parameters; and 3) optimization purpose. In general, single-motor and multispeed or multimotor and multispeed powertrain systems are more complex and have lower transmission efficiency than the previous powertrain systems. However, many studies have been conducted on the optimization of such powertrain systems because of their potential to enhance both EV efficiency and performance [4]. Moreover, while these systems are more expensive to manufacture motors and transmissions than conventional powertrain systems, they can reduce battery capacity and charging costs by enhancing EV energy efficiency, which can be advantageous in terms of the overall electricity cost of EVs [5], [6].

Regarding single-motor and multispeed systems to improve energy efficiency or dynamic performance, several studies have been conducted on the design optimization of transmission parameters, such as gear ratios (GRs) [7], [8], [9], [10], [11], [12] and shift patterns (SPs) [7], [8], [9], [11], [12], [13]; however, these studies have not considered the motor design. In addition, optimizing both motor and transmission parameters, such as maximum motor torque and speed and transmission GRs, has also been studied to improve efficiency and performance [14]. However, there was no specific information regarding motor design for efficiency characteristics, and only the motor torque and speed characteristics were provided. It is worth noting that these

Manuscript received 22 March 2024; revised 20 May 2024; accepted 14 June 2024. Date of publication 18 June 2024; date of current version 3 February 2025. This work was supported by the Basic Science Research Program through the National Research Foundation of Korea (NRF), Ministry of Education, under Grant RS-2023-00239986. *(Kihan Kwon and Dong-Min Kim contributed equally to this work.) (Corresponding author: Seungjae Min.)*

Kihan Kwon is with the Department of Mechanical Design Engineering, Jeonbuk National University, Jeonju 54896, South Korea.

Dong-Min Kim is with the Department of Automotive Engineering, Honam University, Gwangju 62399, South Korea.

Kyoung-Soo Cha is with Korea Institute of Industrial Technology, Daegu 42994, South Korea.

Junhyeong Jo, Myung-Seop Lim, and Seungjae Min are with the Department of Automotive Engineering (Automotive-Computer Convergence), Hanyang University, Seoul 04763, South Korea (e-mail: seungjae@hanyang.ac.kr).

Digital Object Identifier 10.1109/TTE.2024.3416173

characteristics were determined via detailed motor design specifications, such as stack length, number of coil turns, and stator and rotor shapes.

The superiority in terms of efficiency and performance of multimotor and multispeed EVs compared with single-motor and single-speed and multispeed EVs has been demonstrated [15]. However, it is difficult to determine its optimal design, because the powertrain system in that study is more complex than other systems. To address this problem, several previous studies have presented optimization results for a multimotor and multispeed system for energy efficiency improvement, including GRs [16], [17], [18] or SPs [18], [19], [20], [21] optimization for transmissions and torque distribution (TD) or maximum torque characteristic optimization for motors [18], [19], [20], [21], [22]. However, these results did not include specific information regarding motor design for efficiency characteristics. A detailed review of previous works related to EV powertrain system design optimization is summarized in Table I.

This review of the existing literature suggests the following. Unlike previous research trends, several studies have been recently conducted on EVs using multimotor and multispeed systems as much as single-motor and multispeed systems. In addition, GRs and SPs have been commonly adopted in the optimization of transmission design; however, although motors generally have various design parameters compared with transmissions, design variables for motor optimization have not been considered as diverse as transmissions. Moreover, the transmission characteristics represented by them are sufficiently appropriate for EV efficiency and performance analysis; however, while motor characteristics that affect EV efficiency and performance, such as motor efficiency and maximum motor torque curve, are determined via detailed motor design specifications, previous studies on EV system optimization have not considered specific motor designs for these motor characteristics. Therefore, to enhance the practical use of design optimization results, the optimization including the specific motor design for the powertrain system should be performed.

Among multimotor and multispeed powertrain systems for EVs, nonshifting powertrain systems, which have the same number of motors and gear sets, have advantages over shifting powertrain systems. In the case of shifting systems for EVs, the torque interruption during gear shifting causes poor drivability issues, and the additional components for gear shifting, such as the clutch and actuator, contribute to low transmission efficiency [23]. However, nonshifting systems enable no torque interruption by connecting each motor to each speed gear and achieve high transmission efficiency, because there are no separate shifting devices [15]. Therefore, this study focused on a two-motor and two-speed powertrain system to represent multimotor and multispeed powertrain systems for EVs.

Based on the literature review, it is effective to select the TD between motors and the GRs as the design variables for the system optimization. Furthermore, there is a limitation that previous studies failed to focus on specific motor designs and only utilized predefined motor characteristics. Therefore, the detailed motor design specifications, such as stack length, number of coil turns, and stator and rotor shapes, should be reflected in the analysis of motor characteristics to propose a practical and suitable motor design. In this respect, several studies have been conducted to improve the energy efficiency of EVs by optimizing specific aspects of motor design, such as the permanent-magnet motor topologies [24], the size of stator core and permanent magnet [25], and the slot and magnet dimensions [26]. However, these studies only considered the motor optimization, without including the transmission, and focused on single-motor and single-speed EVs. In summary, it is desirable to simultaneously consider the motor TD, GRs, and specific motor design as the design variables for optimizing multimotor and multispeed powertrain systems. In addition, it is worth noting that the SPs were not considered in the nonshifting system, which has the same number of motors and gear sets in this study.

An optimal design solution should provide excellent efficiency and performance. Unfortunately, because of the trade-off relationship between efficiency and performance [27], it is challenging to improve them both. Accordingly, it is necessary to obtain various design solutions optimized for each stipulated requirement. Previous studies show the results of optimizing multimotor and multispeed powertrains for EV efficiency and performance. However, these studies provided different optimal design solutions for each objective [28], or the solutions were obtained using the fixed weight factors for efficiency and performance [8], [14]. Therefore, it is appropriate to implement a multiobjective optimization for handling the trade-off relationship by providing a Pareto front, which contains diverse optimal design solutions [29], [30]. However, because multiobjective optimization typically requires excessive computational effort, multiobjective optimization methods using surrogate models have been suggested for reducing the computational cost in the various vehicle design fields, including the gears for power split device [31], the hydropneumatic suspension [32], and the beam structure for crashworthiness [33]. Among various surrogate models, artificial neural networks (ANNs) using adaptive modeling methods have advantages in ensuring the accuracy and efficiency of ANN models [34].

To address these issues, this study proposes a multiobjective optimization method for a nonshifting EV with a two-motor and two-speed powertrain system, considering a specific motor design. For the analysis of motor characteristics, a finite-element analysis (FEA) was performed using a high-fidelity motor model. The motor analysis model was validated by comparing the FEA and experimental results of the motor efficiency. Using these motor characteristics, a two-motor and two-speed EV model was built to analyze the quantitative measures of EV efficiency and performance. In addition, to improve these objective measures, a multiobjective optimization problem was formulated, including design variables, such as stack length, number of coil turns, and TD coefficient for two motors, and the GR of each speed for two-speed transmission. To effectively solve this optimization

TABLE I
PREVIOUS RESEARCH ON EV MOTOR AND TRANSMISSION SYSTEM OPTIMIZATION (TC: MAXIMUM TORQUE CHARACTERISTIC, TD: TORQUE DISTRIBUTION, GR: GEAR RATIO, AND SP: SHIFT PATTERN)

Reference	Year	System		Optimization			
				Variable		Objective	
		Motor	Speed	Motor	Transmission	Efficiency	Performance
Li et al. [14]	2020	1	2	TC	GR	◯	◯
Ahssan et al. [7]	2020	1	2		GR,SP	◯	◯
Sun et al. [8]	2021	1	2		GR,SP	◯	◯
Kwon et al. [9]	2021	1	2		GR,SP	◯	◯
Wu et al. [10]	2022	1	3		GR	◯	◯
Liu et al. [13]	2022	1	2		SP	◯	
Zhang et al. [11]	2022	1	2		GR,SP	◯	
Kwon et al. [12]	2023	1	2		GR,SP	◯	◯
Zhao et al. [19]	2019	2	2	TD	SP	◯	
Kwon et al. [16]	2020	2	2	TD	GR	◯	◯
Nguyen et al. [22]	2021	2	4	TD	SP	◯	
Nguyen et al. [17]	2022	2	2		GR	◯	◯
Yu et al. [20]	2022	2	4	TD	SP	◯	
Kwon et al. [18]	2023	2	2,3,4	TD	GR,SP	◯	◯
Yu et al. [21]	2023	2	2	TD	SP	◯	

problem, an ANN model for EV efficiency and performance was developed. From the ANN-model-based optimization results, the Pareto optimal solutions were obtained. The design solutions in the Pareto front exhibited a trade-off between efficiency and performance and provided specific optimal motor designs. In addition, the optimization results present an improvement in both efficiency and performance compared with reference vehicles, which consist of single-motor and single-speed or multispeed powertrain systems. Finally, a comparison between the computational effort and error of the ANN and vehicle models demonstrates the validity of multiobjective optimization using the ANN model. The main contributions of this study are summarized as follows.

1) Although the motor characteristics based on the motor design analysis significantly affect EV efficiency and performance, previous studies on optimizing multimotor and multispeed EVs have not considered their importance. To address this point, this study analyzed the motor characteristics and the effect of motor design parameters to demonstrate the importance of considering specific motor design parameters for the design optimization of EVs.
2) Unlike the previous studies, this study considered the specific motor design parameters as the design variables in the multiobjective optimization process. In addition, the comparison according to the optimization of motor and transmission was presented to highlight the effectiveness of motor design optimization in the multimotor and multispeed EVs.
3) To compare the optimization results among the various EV powertrain systems, the optimizations of these systems were performed using the ANN-based multiobjective optimization process. The comparison of efficiency and performance quantitatively demonstrates the superiority of two-motor and two-speed EVs, and the distribution results of motor design solutions exhibit the importance of the design considering motor characteristics.

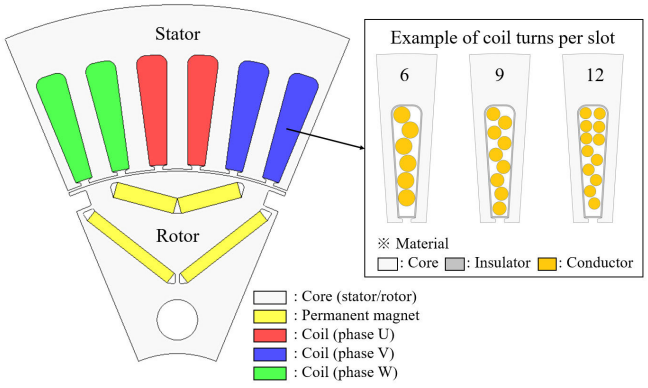

Fig. 1. Reference motor design (1/8 model).

II. ANALYSIS MODEL

For an analysis of the energy efficiency and dynamic performance of the EV, this study adopted an EV powertrain system, including two-motor and two-speed transmission. The motor and EV analyses are performed using a high-fidelity finite-element model (by JMAG) and a 1-D functional model (by MATLAB/Simulink), respectively. The details of the motor and EV models are presented next.

A. Motor Model

To consider a specific motor design, the FEA-based high-fidelity motor model was developed. This model calculates the motor torque and efficiency according to the design specifications. The reference motor is an interior permanent-magnet synchronous motor (IPMSM) based on a commercial

TABLE II
REFERENCE MOTOR SPECIFICATIONS

Item	Specification
Pole/Slot number	8/48
Stator/Rotor diameter	200/126 mm
Stack length	150 mm
Coil turns	18
Nominal voltage	360 V
Maximum power	80 kW
Maximum torque	270 Nm
Base/Maximum speed	2700/10000 RPM

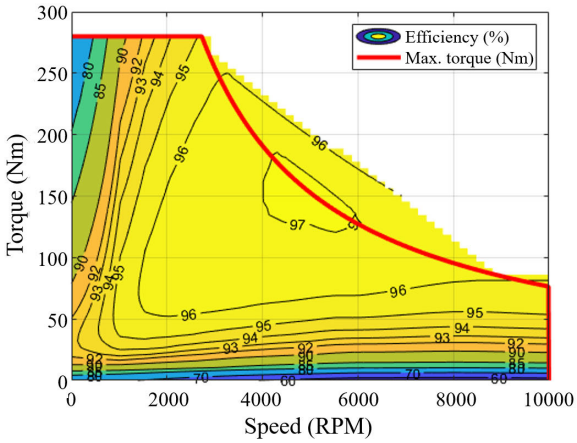

Fig. 2. Reference motor operational characteristics.

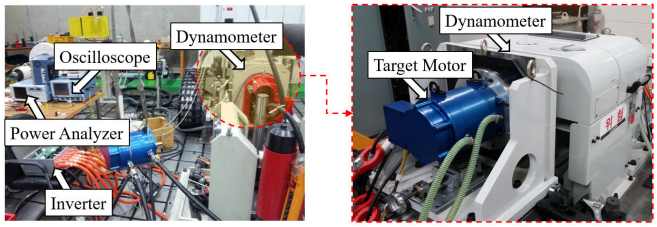

Fig. 3. Configuration for the motor experiment.

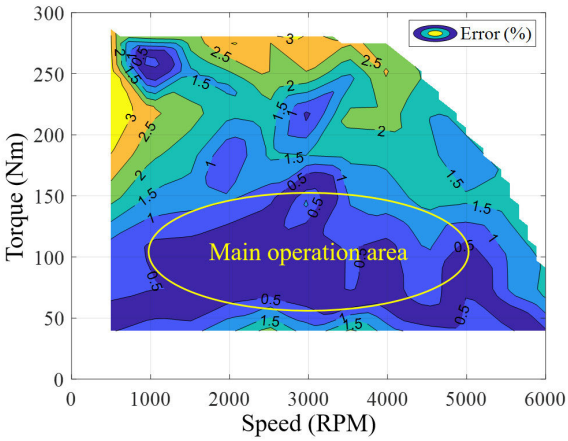

Fig. 4. Efficiency error between the FEA and experiment results.

motor employed in the Nissan Leaf EV; the motor is shown in Fig. 1, and its specifications are summarized in Table II. The motor torque (T_m) is expressed as follows:

$$T_m = p_n\left[\phi_f i_q + \left(L_d - L_q\right) i_d i_q\right] \tag{1}$$

where p_n is the number of pole pairs, ϕ_f is the flux linkage by field, L_d and i_d are the d-axis inductance and current, respectively, and L_q and i_q are the q-axis inductance and current, respectively. Here, the ϕ_f, L_d, and L_q are determined from the FEA result, and the i_d and i_q are defined by the motor voltage equations of the d- and q-axes [35].

Then, the motor efficiency (η_m) is determined using the copper (W_c) and iron (W_i) losses as follows:

$$\eta_m = \frac{T_m \omega_m}{T_m \omega_m + W_c + W_i} \tag{2}$$

where ω_m is the motor speed. Here, W_i is derived from the FEA result, and W_c is expressed as follows:

$$W_c = R_w\left(i_d^2 + i_q^2\right) \tag{3}$$

where R_w is the motor winding resistance. From (1) and (2), the maximum motor torque curve and efficiency map are obtained, as shown in Fig. 2.

To verify the analytical results, the experimental setup for the fabricated motor was prepared, as shown in Fig. 3. The dynamometer and the test motor were coupled to an in-line torque sensor from Kistler at both ends. The test motor was connected to an inverter supplied by a driver command (DC) power source, and the motor input power was measured by connecting YOKOGAWA's power analyzer WT3000 in a three-phase four-wire method. The water jacket of the motor was supplied as cooling water using a hose connected with a chiller to the water pump to maintain the test conditions. Based on this test bench, the motor efficiency measurement was conducted in the following procedure.

1) Rotating the dynamometer as desired test speed.
2) Input three-phase current to the test motor to output desired test torque.
3) Measure the input power and torque through the power meter and torque sensor, respectively.
4) Step up the desired test speed and torque and repeat 1)–3).
5) Calculate the efficiency of all the test points based on the measured input power, torque, and speed.

Fig. 4 shows the efficiency error between the motor FEA and experimental results. Because the overall error in the main operation area under standard driving cycles (e.g., UDDS, NEDC, or WLTP) is less than 0.5%, the utilized FEA model is suitable for analyzing the motor characteristics. Therefore, to analyze the two-motor and two-speed EVs, the maximum torque, speed, and efficiency of each motor were calculated using the FEA model. Each motor characteristic was used for the vehicle model described in Section II-B.

B. Vehicle Model

From the input DC, the vehicle model calculates the electricity consumption per 100 km (EC100) and vehicle speed to evaluate the energy efficiency and dynamic performance, respectively. The DC value is determined to be within ±1,

and a positive or negative DC value indicates the vehicle acceleration or braking, respectively. Under the vehicle acceleration conditions (DC $>$ 0), the output torque request (T_{req}) is expressed as follows:

$$T_{\text{req}} = (T_{\text{max1}} r_1 + T_{\text{max2}} r_2) \cdot \text{DC} \tag{4}$$

where T_{max1} and T_{max2} are the maximum torque of each motor, which depends on the motor speed, and r_1 and r_2 are the total GRs for each speed, the values of which are calculated by multiplying the speed GR by the final GR. The vehicle power request (P_{req}) is determined using T_{req} and v as follows:

$$P_{\text{req}} = \frac{T_{\text{req}}}{R_t} v \tag{5}$$

where R_t is the effective tire radius and v is the vehicle speed. Because the summation of each motor power, which is defined by multiplying the motor speed by its torque, should be equal to P_{req}, each motor torque (T_1 and T_2) is determined using the TD coefficient (c_m) as follows:

$$\begin{aligned} T_1 &= c_m T_{\text{max1}} \\ T_2 &= \frac{P_{\text{req}} - T_1 \omega_1}{\omega_2} \end{aligned} \tag{6}$$

where ω_1 and ω_2 represent the speed of each motor. Here, c_m is determined so as to maximize both motor efficiencies and ranges from 0 to 1; $c_m = 0$ or 1 means that the first motor torque is zero or maximum, respectively. When each motor torque is determined, the output torque (T_{out}) can be calculated as follows:

$$T_{\text{out}} = \eta_t (T_1 r_1 + T_2 r_2) \tag{7}$$

where η_t is the transmission efficiency. In general, the transmission efficiency varies with input torque and speed. However, almost all transmission losses occur from the gear-shift devices. Since the transmission structure employed in this study is a nonshift device type, the transmission efficiency variation is slight compared with the motor efficiency variation according to torque and speed. Therefore, η_t is considered a constant value. To calculate the vehicle speed, the resistance and braking torque, as well as the output torque, should be analyzed. First, the resistance torque (T_{res}) is derived by the air, rolling, and climbing resistances as follows:

$$T_{\text{res}} = -\left[\frac{1}{2} c_d \rho A v^2 + Mg(\mu_r \cos\theta + \sin\theta)\right] R_t \tag{8}$$

where c_d is the drag coefficient, ρ is the air density, A is the frontal area, M is the total vehicle mass, g is the gravitational acceleration, μ_r is the rolling friction coefficient, and θ is the road gradient. Second, the braking torque consists of the mechanical and regenerative torque. Under the vehicle braking conditions (DC $<$ 0), the braking torque (T_{brk}) is expressed as follows:

$$T_{\text{brk}} = C_{\text{brk}} \cdot \text{DC} \tag{9}$$

where C_{brk} is the maximum braking torque capacity. When the motors are regenerated, T_{brk} is divided into the mechanical braking torque ($T_{\text{brk}.m}$), and both regeneration motor torques as follows:

$$T_{\text{brk}} = T_{\text{brk}.m} + (T_1 r_1 + T_2 r_2). \tag{10}$$

Here, both motor torques (T_1 and T_2) are determined using (6). From T_{out}, T_{res}, and T_{brk}, the wheel speed (ω_{whl}) is determined as follows:

$$\dot{\omega}_{\text{whl}} = \frac{T_{\text{out}} + T_{\text{res}} + T_{\text{brk}}}{J_{\text{eq}}} \tag{11}$$

where J_{eq} is the equivalent vehicle inertia, which consists of the powertrain, wheel, and vehicle mass inertias. From ω_{whl}, v is expressed to evaluate the dynamic performance of the vehicle as follows:

$$v = R_t \int \dot{\omega}_{\text{whl}} dt. \tag{12}$$

To measure EC100, which represents energy efficiency, the value of the battery state of charge (SOC) is used. First, the SOC consumption (ΔSOC) is calculated using a battery equivalent circuit model as follows:

$$V_b = V_o - R_i I_b \tag{13}$$

where V_b and V_o are the battery and open-circuit voltages, respectively; R_i is the internal resistance, and I_b is the battery current. Here, I_b is derived using each motor power according to the battery charging or discharging condition as follows:

$$I_b = \begin{cases} \left(\dfrac{T_1\omega_1}{\eta_1} + \dfrac{T_2\omega_2}{\eta_2}\right)\dfrac{1}{\eta_i V_b} & \text{if } T_{\text{out}} \geq 0 \text{ (discharging)} \\ \dfrac{\eta_1 T_1 \omega_1 + \eta_2 T_2 \omega_1}{V_b}\eta_i & \text{if } T_{\text{out}} < 0 \text{ (charging)} \end{cases} \tag{14}$$

where η_1 and η_2 represent the efficiency of each motor, which depends on the motor torque and speed, and η_i is the constant inverter efficiency. This study considers an ideal inverter model that regularly supplies ac to the motor and has a constant efficiency, because the variation in the motor efficiency is significantly larger than that of the inverter. Then, ΔSOC can be determined by integrating I_b as follows:

$$\Delta\text{SOC} = \frac{\int I_b dt}{C_{\text{bat}}} \tag{15}$$

where C_{bat} is the energy capacity of the battery. The value of EC100, meaning the electricity consumption per 100 km of EVs, can be determined using the value of ΔSOC under standard driving cycles as follows:

$$\text{EC100} = \frac{C_{\text{bat}} \cdot \Delta\text{SOC}}{d_{\text{cyc}}} \times 100 \tag{16}$$

where d_{cyc} is the distance of the standard driving cycle (km). The parameter values of the reference EV used in this study are summarized in Table III [36].

TABLE III
REFERENCE VEHICLE SPECIFICATIONS

Item		Specification
Vehicle mass		1,600 kg
Frontal area		2.27 m^2
Drag coefficient		0.29
Rolling friction coefficient		0.01
Tire radius		0.31 m
Total gear ratio		7.940
Battery	Voltage	360 V
	Capacity	24 kWh

III. EFFECT OF MOTOR DESIGN PARAMETERS ON MOTOR CHARACTERISTICS

Although high motor torque and efficiency provide the advantages of improved EV driving performance and energy efficiency, respectively, it is difficult to achieve both characteristics in motor design. Therefore, it is necessary to analyze the effect of motor design parameters on motor characteristics to determine the optimal motor design. In particular, the maximum motor torque and efficiency characteristics, as shown in Fig. 2, directly affect EV performance and efficiency. Moreover, these characteristics vary with the motor design parameters, such as stack length, number of coil turns, and stator and rotor shape. In practical motor design, the stack length and number of coil turns are easier to modify in the original motor design than the stator and rotor shape. Accordingly, this study analyzes the motor characteristics according to the variations in stack length and number of coil turns.

To analyze the effect of stack length and number of coil turns on the motor characteristics, it is necessary to determine the available design range of both parameters. In terms of stack length, a long length can ensure a high maximum motor torque; however, it increases the motor cost and mass. Because the stack length of the reference motor is 150 mm, as shown in Table II, the sum of the lengths of the two motors is limited to this value. Conversely, an excessively short length causes durability and manufacturing problems. In addition, end leakage flux occurs largely in small shape ratio motors [37]. It means that the torque density can be reduced if the stack length is too short with the same cross-sectional area. Therefore, too short stack length results in a small shape ratio, which should be avoided. For this reason, this study considers the minimum stack length of the motor to be 50 mm. This means that the stack length should range between 50 and 100 mm. An example of the stack length for each motor is shown in Fig. 5.

In terms of the number of coil turns, an increase in turns can reduce the line current when maintaining magnetomotive force from the armature. In addition, it can increase the line-to-line voltage; however, this leads to a decrease in motor efficiency from flux weakening control for the high-speed operation region. Fig. 6 shows the analysis results of the motor torque and line current along to the coil turns at the motor base speed (2700 RPM). To guarantee the maximum motor power

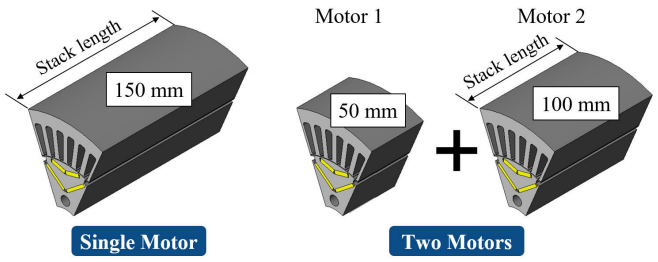

Fig. 5. Example of stack length for a single- and dual-motor.

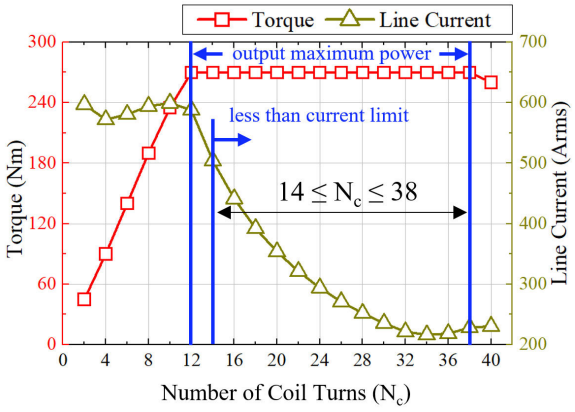

Fig. 6. Analysis result of motor torque and line current at a base speed of 2700 RPM.

and to be less than the limited line current, the coil turns should range from 14 to 38 turns. At this time, base speed is the maximum speed at which maximum torque can be produced, and at the same time, it is the minimum speed at which the line-to-line voltage is used to its maximum value, and at the same time, it is the speed at which maximum output begins to be produced. Therefore, we investigated the motor characteristics for the base speed and determined the range of the number of coil turns.

Based on these design ranges, the effect of design parameters on the motor characteristics, such as the maximum torque curve and efficiency map, was analyzed, as shown in Fig. 7. The motor characteristics analysis was performed up to 15 000 RPM to consider a wide range of motor operation conditions despite the decrease in motor power at extremely high speeds. As a result, first, the stack length and coil turns directly affect the maximum motor torque. Because the stack length is proportional to the amount of flux linkage, it is related to the magnetic flux within the motor. In addition, an increase in coil turns increases the magnetomotive force within the motor. Therefore, the maximum motor torque is proportional to the stack length and coil turns. Second, the coil turns have a significant effect on the motor efficiency compared with the stack length. An increase in coil turns leads to a large amount of current within the motor, resulting in a large copper loss in the overall motor operating area. Therefore, the average motor efficiency depends on the coil turns. In addition, the stack length can vary the distribution of motor efficiency, because it affects the resistance of the motor.

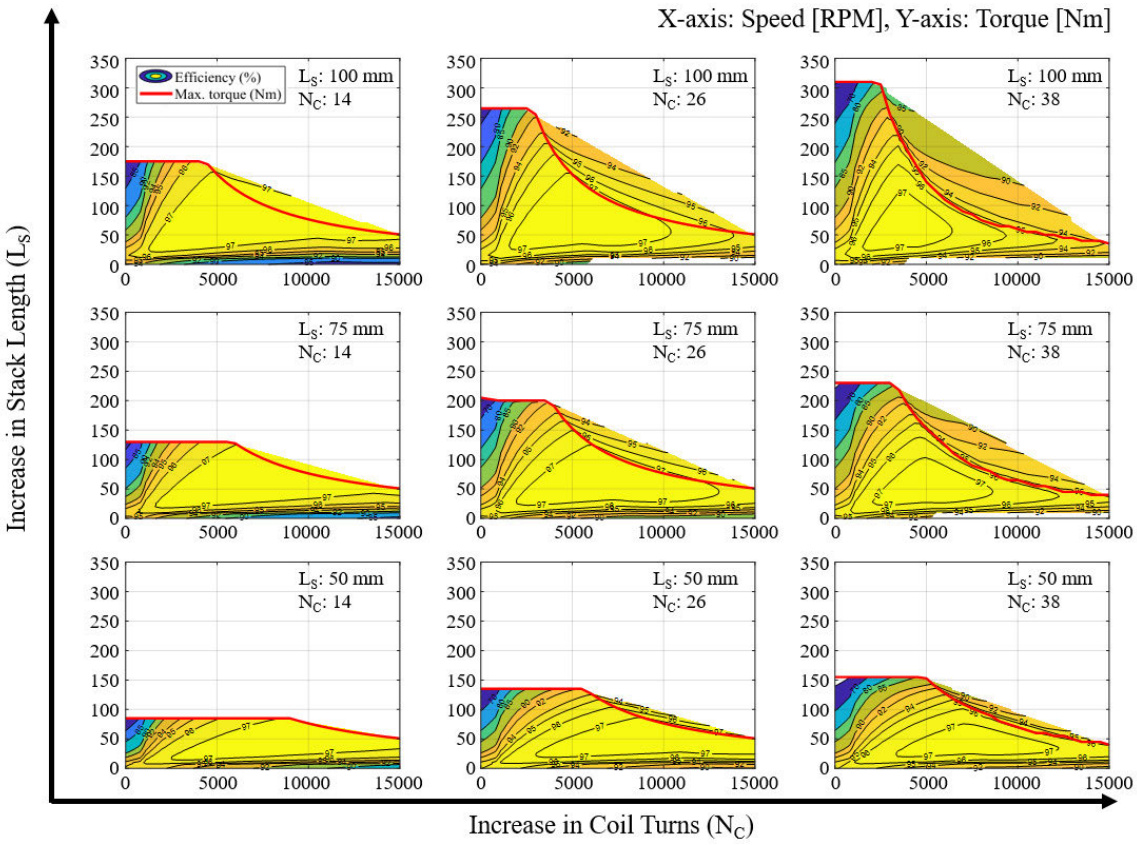

Fig. 7. Effect of design parameters on motor characteristics.

Accordingly, both parameters are significantly related to the motor characteristics.

These motor characteristics are directly involved in the energy efficiency and dynamic performance of the EV. Moreover, in two-motor and two-speed powertrain systems, the TD between the two motors and the GRs can adjust the motor operating points and multiply the motor torque [16]. Therefore, these parameters should be appropriately determined to operate the motors in the high-efficiency area and to output a high traction force. In summary, to maximize both EV efficiency and performance, the motor design parameters, such as stack length and number of coil turns, should be determined by considering the optimal TD and GRs.

IV. Multiobjective Optimization Process

To evaluate the design requirements of EV, a requirement quantification should be determined. This study used the EC100 from the WLTP driving cycle for the energy efficiency and the acceleration time (t_{acc}) of 0–100 km/h under maximum accelerating condition for the dynamic performance. Details of the optimization process are presented next.

A. Optimization Problem Formulation

In the EV design optimization process, using multiobjective optimization method is more appropriate than single-objective optimization, because it can handle the trade-off between the efficiency and performance of EVs. For the design optimization of two-motor and two-speed transmission EVs, the design variables are the stack length, number of coil turns, and TD coefficient for motors, and the GR of each speed for transmission. Considering this, the multiobjective optimization problem can be formulated as follows:

$$\begin{aligned} &\underset{x}{\text{minimize}} \quad f(\mathbf{x}) = \bar{f}(\text{EC100}, t_{\text{acc}}) \\ &\text{s. t.} \quad \mathbf{x} \in \Omega_c \\ &\qquad \text{where} \quad \mathbf{x} = [\mathbf{L}, \mathbf{N}, \mathbf{r}, \mathbf{C}] \end{aligned} \tag{17}$$

where $\mathbf{L} = [L_s^1, L_s^2]$ and $\mathbf{N} = [N_c^1, N_c^2]$ are the stack length and number of coil turns sets, respectively; $\mathbf{r} = [r_1, r_2]$ is the GR set, $\mathbf{C}$ is the matrix of the optimal TD coefficients (c_m) depending on the vehicle speed (v) and DC, and Ω_c represents the design variable constraints, such as the upper and lower bounds of the stack length and the number of coil turns and the dynamic constraints of the GRs. Here, because a coil should be paired with another coil and the coil turns are an integer value, the design variable $\mathbf{N}$ is accepted as an even number within the optimization process. Therefore, $\mathbf{L}$, $\mathbf{C}$, and $\mathbf{r}$ are the continuous variables, while $\mathbf{N}$ is the discrete variable in this optimization.

To update $\mathbf{C}$ for each iteration, the optimization process involves a suboptimization process that optimizes the TD coefficients [16]. For a certain combination of design variables ($\mathbf{L}$, $\mathbf{N}$, and $\mathbf{r}$), the TD coefficients can be optimized for minimizing energy consumption. Therefore, to solve (17), the optimization is performed separately for $\mathbf{C}$ and for the

other design variables (**L**, **N**, and **r**). To derive the optimal TD coefficients, a suboptimization problem is formulated as follows:

$$\begin{aligned} &\underset{c_m}{\text{minimize}} \quad f(c_m) = \frac{T_1(c_m)\omega_1}{\eta_1} + \frac{T_2(c_m)\omega_2}{\eta_2} \\ &\text{s. t.} \quad T_1\omega_1 + T_2\omega_2 = P_{\text{req}}(v, \text{DC}). \end{aligned} \tag{18}$$

For the motor design, **L** and **N** constraints are as follows:

$$\begin{aligned} &50 \le \mathbf{L} \le 100 \\ &\sum \mathbf{L} = 150 \\ &14 \le \mathbf{N} \le 38. \end{aligned} \tag{19}$$

To determine the feasible region of each GR (r_1 and r_2), the dynamic constraints should be considered so as to meet the basic driving requirements of EVs [9]. Because the dynamic performance objective is 0–100-km/h acceleration, both motors are required to drive until the vehicle is accelerated to 100 km/h. Therefore, the maximum value of the first GR ($\bar{r}_{1\max}$) is determined by considering the maximum motor speed ($\omega_{\max}$) as follows:

$$\bar{r}_{1\max} = \frac{\omega_{\max} \cdot R_t}{100/3.6}. \tag{20}$$

Since the first GR is always greater than the second GR ($r_1 > r_2$), when driving at the maximum speed of the EV, the second motor is only operating. Therefore, the maximum value of the second GR ($\bar{r}_{2\max}$) can be determined by considering the demanded maximum vehicle speed ($\bar{v}_{\max}$) and the maximum motor speed ($\omega_{\max}$) as follows:

$$\bar{r}_{2\max} = \frac{\omega_{\max} \cdot R_t}{\bar{v}_{\max}/3.6}. \tag{21}$$

Here, the $\bar{v}_{\max}$ is set to 150 km/h considering the reference vehicle specifications. Furthermore, the traction force at maximum vehicle speed should be greater than the resistance force induced by air and rolling drag. For this reason, the minimum second GR ($\bar{r}_{2\min}$) is determined by considering the resistance force as follows:

$$\bar{r}_{2\min} = \frac{R_t\left(\mu_r Mg + \frac{1}{2}c_d\rho A\bar{v}_{\max}^2\right)}{T_{\max 2}}. \tag{22}$$

Here, the value of $T_{\max 2}$ is the torque at the maximum motor speed for a motor designed with the maximum stack length and the number of coil turns ($L_s = 100$ and $N_c = 38$), because such conditions output the minimum torque at the maximum motor speed among all motor design candidates, as shown in Fig. 7.

B. ANN Modeling

In general, multiobjective optimization entails a high calculation burden, as opposed to single-objective optimization. To address this problem, ANN-based multiobjective optimization has been performed to decrease the computational burden in the optimization of various vehicle designs. ANN models can predict complex and nonlinear relationships between system input and output [38]. Therefore, this study employs an ANN model built using the neural network toolbox available in MATLAB. For the ANN model construction, the design variables (**L**, **N**, and **r**) and objective functions (EC100 and t_{acc}) were selected as model inputs and outputs, respectively. The ANN model configuration is as shown in Fig. 8, and the parameter settings are summarized in Table IV.

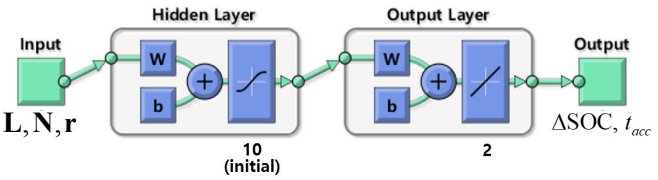

Fig. 8. ANN model configuration.

TABLE IV
ANN MODEL PARAMETERS

Parameter		Setting
Sample percentage	Training	70%
	Validation	15%
	Testing	15%
Initial hidden layer nodes		10
Output layer nodes		2
Activation function		Sigmoid
Training algorithm		Bayesian regularization

The ANN model should achieve high model accuracy with as little computational effort as possible [39]. To improve model accuracy, in addition to increasing the number of samples, a large number of hidden layer nodes are required within the ANN model; however, increasing the number of samples can be a burden to build the ANN model, and increasing the number of nodes can lead to overfitting problems and excessive training times. Accordingly, it is acceptable to use the least possible samples and nodes to ensure target model accuracy in the ANN-based modeling process. To determine the suitable number of samples and nodes, this study utilizes an effective modeling method that continuously validates the model accuracy while reconstructing the ANN model and gradually increasing the number of samples and nodes [34].

The ANN modeling process is shown in Fig. 9. First, the initial samples are selected using the optimal Latin hypercube design (OLHD) [40], and the ANN model for the objective functions is constructed. To quantify the model accuracy, the normalized root-mean-square error (NRMSE) is utilized by performing a cross-validation-based comparison between the objective function values from the vehicle and ANN models. Next, if the calculated NRMSE of the ANN model is greater than the demanded NRMSE, a new set of samples is appended to the current samples. In this stage, the number of hidden layer nodes can increase when the rate of difference in NRMSE between the current and previous values is significantly low to improve the prediction accuracy of the ANN model. In addition, the new sample points are determined to evenly encompass the feasible design regions using the maximin distance design (MDD) [41]. Whenever the number of samples and nodes increases, this process

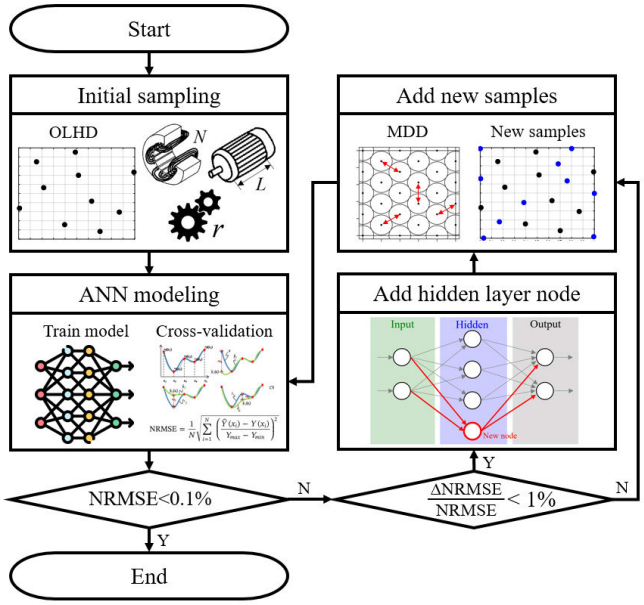

Fig. 9. ANN modeling process.

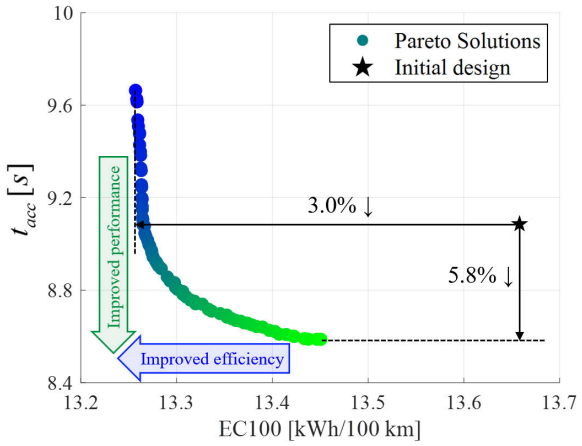

Fig. 10. Pareto front solutions.

repeatedly computes the NRMSE and is terminated when the new NRMSE is less than 0.1%. Finally, an ANN model is developed using the samples and nodes from the current step. As a result of applying this process, the ANN model for the objective functions (EC100 and t_{acc}) was constructed using 178 samples with 20 nodes.

V. Optimization Results

Based on the ANN model of the objective functions representing EC100 and t_{acc}, the optimization problem formulated in (17) was solved using the NSGA-II algorithm [42], which has advantages in solving nonlinear functions and multiobjective optimization problems, and obtained the optimization results. The initial design parameters were employed as follows: the stack length for each motor is the same as 75 mm without optimal TD, the number of coil turns for each motor is the same as 18 by referring to Table II, and the GRs for each speed are 11.91 and 7.94 for the first- and second-speed, respectively, using the GR of the reference vehicle (Table III) and 1.5 step ratio. A Pareto front, comprising of 70 optimal solutions for EC100 and t_{acc}, is shown in Fig. 10. This result indicates a balanced relationship between the two objectives, representing a trade-off between EV efficiency and performance. In addition, a comparison of results between the initial design and the Pareto optimal solutions exhibits that EC100 and t_{acc} can be improved by up to 3.0% and 5.8%, respectively.

Fig. 11 shows the optimal solution distributions for the optimal design solutions at the Pareto front. The Pareto front and optimal design solutions were displayed using the gradation effect to match the design solutions corresponding to the objective function values. The solution close to the blue or light-greed color means that it is beneficial to efficiency or performance, respectively. The effect of each design variable on the objective functions can be identified from the results of the design solutions. For stack length, a similar length for each motor is advantageous in terms of energy efficiency. Conversely, a long first motor length (and a short second motor length) is advantageous in terms of acceleration performance. Because the GR with the first motor is large and the stack length is proportional to the maximum torque, the first motor length affects the acceleration time more than the second motor length. For the number of coil turns, a small or large number of turns is advantageous in terms of efficiency or performance, respectively. As shown in Fig. 7, a small and large number of coil turns offer advantages in terms of motor efficiency and maximum torque, respectively. In particular, the first motor is significantly related to acceleration time, because a large number of coil turns are in the range of small acceleration times, whereas the second motor is more significantly related to energy efficiency than the first motor. For the GRs, small or large ratios are desirable for efficiency or performance, respectively. Because superior energy efficiency and dynamic performance rely on the combination of motors and GRs, the effect of GR on the objectives should be analyzed considering the motor characteristics, such as the efficiency distribution and maximum motor torque. Accordingly, because the various design variables, such as stack length, number of coil turns, TD, and GRs, affect both objectives, an effective optimization method should be implemented to achieve maximum efficiency and performance of EVs. In addition, these results, including the various design solutions for each weighted objective, demonstrate the importance of multiobjective optimization to obtain the most appropriate design solutions depending on each engineer's requirements.

To confirm the importance of considering motor design parameters that affect motor characteristics, the system optimization results are compared, as shown in Fig. 12: 1) including motor design variables and 2) fixed motor design parameters (see Table II, $\mathbf{L} = 75$ and $\mathbf{N} = 18$). These results demonstrate the effectiveness of the system optimization, including motor design parameters, because the EC100 and t_{acc} are further improved. Therefore, the optimization considering specific motor designs is appropriate in the design of multimotor and multispeed powertrain systems

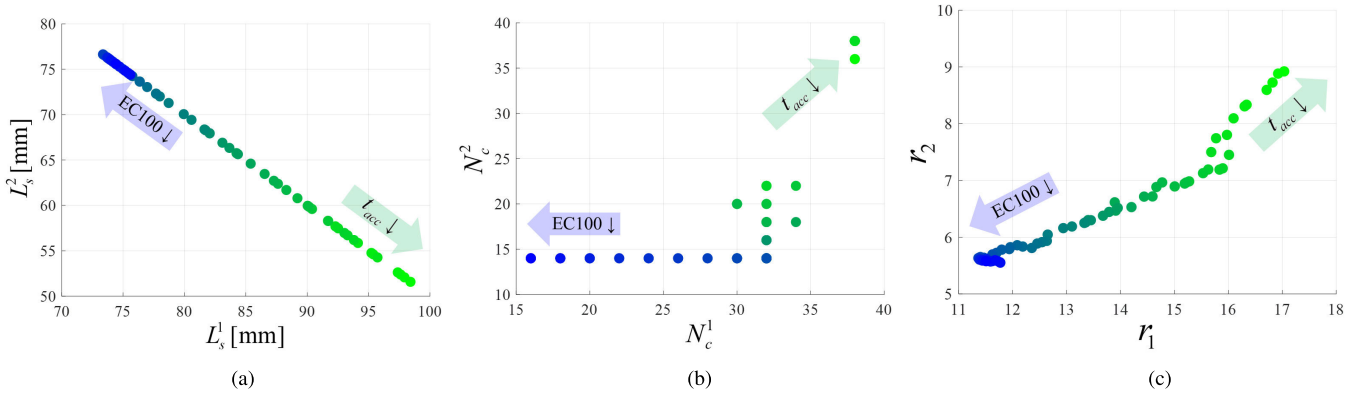

Fig. 11. Distributions of optimal solutions for each design variable. (a) Stack length (L_s^1 and L_s^2). (b) Coil turns (N_c^1 and N_c^2). (c) GR (r_1 and r_2).

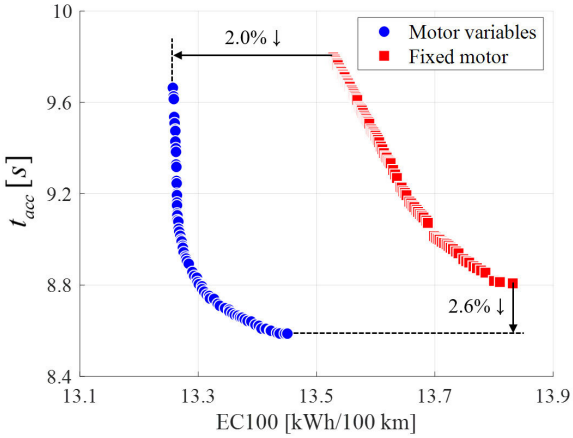

Fig. 12. Comparison according to system optimization results between including motor variables and fixed motor design.

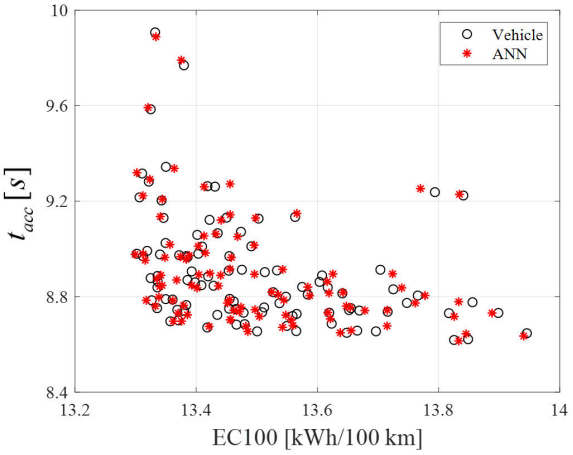

Fig. 14. Comparison of the results between the vehicle and ANN models.

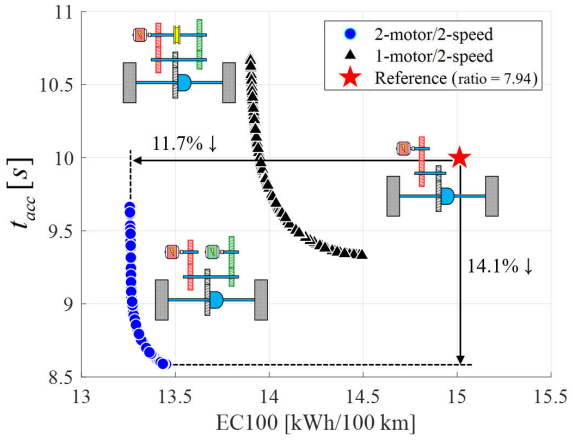

Fig. 13. Comparison between different system design solutions.

to enhance EV efficiency and performance. To confirm the effectiveness of the two-motor and two-speed EV, the optimization results are compared with a reference (single-motor and single-speed EV) and a single-motor and two-speed EV, as shown in Fig. 13. For the optimization of the single-motor and two-speed EV, the GRs and shifting patterns are considered the optimization variables. Here, the optimal GRs and SPs were determined using the method proposed by Kwon et al. [9]. These results clearly demonstrate that the two-motor and two-speed EV outperforms other EVs in terms of dynamic performance and energy efficiency. In addition, the EC100 variation of the Pareto solutions for the single-motor and two-speed EV was significantly greater than that of the two-motor and two-speed EV. Therefore, the two-motor and two-speed EV can enable a more robust design in terms of energy efficiency, because the motor efficiency at the operating points can be improved in a given design through the optimal motor TD, despite the different motor and GR designs. Two-motor and two-speed powertrain systems can achieve excellent performance on EVs; however, they can increase cost and system complexity compared with other powertrain systems. Therefore, the development of multimotor and multispeed powertrain systems requires a comprehensive evaluation of EVs, including these points.

To avoid an excessive computational effort, these optimal design solutions were obtained using the ANN model. Therefore, the prediction accuracy of the constructed ANN model needs to be validated. For the objective functions (EC100 and t_{acc}), this study compared the output values of the vehicle and ANN models for 100 randomly selected design variables in the feasible region, as shown in Fig. 14. Here, the vehicle model results were analyzed using the FEA results

for each motor design variable combination. Since the overall errors for EC100 and t_{acc} are approximately 0.06% and 0.09%, respectively, the accuracy values of the ANN models are considered highly reliable. In addition, approximately 50 000 calculations were required to obtain the Pareto solutions. Therefore, if we directly utilize the motor FEA results to optimize this powertrain system, a required computational time would be expected as 350 days in our computing environment. However, the ANN model enables the calculation of the objective function values without the motor FEA results. It is possible to rapidly calculate the objective function values for repeatedly updated design variables during the multiobjective optimization process. When utilizing the constructed ANN models, the time required to obtain the optimal solutions was only approximately 40 h:36 h for constructing the ANN model and the rest for the optimization. In summary, using the ANN models is highly effective for solving the multiobjective optimization problem for complex vehicle systems.

VI. Conclusion

This article proposed an effective system optimization method for a two-motor and two-speed powertrain EV. The results of the motor parameter effect analysis showed the importance of the specific design of the motor in a multimotor powertrain system. In addition, the optimization results indicated the necessity of optimization considering the effect of specific motor designs on motor characteristics for the powertrain system design of EVs. A comparison of the efficiency and performance results between the reference, single-motor and two-speed, and two-motor and two-speed EVs clearly demonstrated the superiority of the two-motor and two-speed EVs. In future work, the proposed optimization method will be applied to the other EVs, such as three-motor and four-wheel independent drive powertrain systems, to improve the efficiency and performance of EVs, and detailed motor design parameters, such as air gap, magnet dimension, and size of core and armature, will be addressed to further improve EV efficiency and performance.

References

[1] H. He et al., "China's battery electric vehicles lead the world: Achievements in technology system architecture and technological breakthroughs," *Green Energy Intell. Transp.*, vol. 1, no. 1, Jun. 2022, Art. no. 100020.

[2] R. Wang, H. Liu, M.-J. Li, Q. Sun, X. Li, and P. Wang, "Fast charging control method for electric vehicle-to-vehicle energy interaction devices," *IEEE Trans. Transport. Electrific.*, vol. 9, no. 4, pp. 4941–4950, Apr. 2023.

[3] S. Zheng, X. Zhu, Z. Xiang, L. Xu, L. Zhang, and C. H. T. Lee, "Technology trends, challenges, and opportunities of reduced-rare-Earth PM motor for modern electric vehicles," *Green Energy Intell. Transp.*, vol. 1, no. 1, Jun. 2022, Art. no. 100012.

[4] J. Wu, X. Hong, G. Feng, and Y. Zhang, "Seamless mode shift control for a new Simpson planetary gearset based dual motor powertrain in electric vehicles," *Mechanism Mach. Theory*, vol. 178, Dec. 2022, Art. no. 105056.

[5] J. Ruan and Q. Song, "A novel dual-motor two-speed direct drive battery electric vehicle drivetrain," *IEEE Access*, vol. 7, pp. 54330–54342, 2019.

[6] J. Ruan, P. D. Walker, N. Zhang, and J. Wu, "An investigation of hybrid energy storage system in multi-speed electric vehicle," *Energy*, vol. 140, pp. 291–306, Dec. 2017.

[7] M. R. Ahssan, M. Ektesabi, and S. Gorji, "Gear ratio optimization along with a novel gearshift scheduling strategy for a two-speed transmission system in electric vehicle," *Energies*, vol. 13, no. 19, p. 5073, Sep. 2020.

[8] G.-B. Sun, Y.-J. Chiu, W.-Y. Zuo, S. Zhou, J.-C. Gan, and Y. Li, "Transmission ratio optimization of two-speed gearbox in battery electric passenger vehicles," *Adv. Mech. Eng.*, vol. 13, no. 6, Jun. 2021, Art. no. 168781402110228.

[9] K. Kwon, J. Jo, and S. Min, "Multi-objective gear ratio and shifting pattern optimization of multi-speed transmissions for electric vehicles considering variable transmission efficiency," *Energy*, vol. 236, Dec. 2021, Art. no. 121419.

[10] P. Wu, P. Qiang, T. Pan, and H. Zang, "Multi-objective optimization of gear ratios of a seamless three-speed automated manual transmission for electric vehicles considering shift performance," *Energies*, vol. 15, no. 11, p. 4149, Jun. 2022.

[11] W. Zhang, J. Yang, and W. Zhang, "Influence of a new type of two-speed planetary gear automatic transmission on the performance of battery electric vehicles," *Energies*, vol. 15, no. 11, p. 4162, Jun. 2022.

[12] K. Kwon, J.-H. Lee, and S.-K. Lim, "Optimization of multi-speed transmission for electric vehicles based on electrical and mechanical efficiency analysis," *Appl. Energy*, vol. 342, Jul. 2023, Art. no. 121203.

[13] Y. Liu, D. Gao, K. Zhai, Q. Huang, Z. Chen, and Y. Zhang, "Coordinated control strategy for braking and shifting for electric vehicle with two-speed automatic transmission," *eTransportation*, vol. 13, Aug. 2022, Art. no. 100188.

[14] Y. Li, B. Zhu, N. Zhang, H. Peng, and Y. Chen, "Parameters optimization of two-speed powertrain of electric vehicle based on genetic algorithm," *Adv. Mech. Eng.*, vol. 12, no. 1, Jan. 2020, Art. no. 168781402090165.

[15] B. Zhu et al., "Two motor two speed power-train system research of pure electric vehicle," SAE Tech. Paper 2013-01-1480, 2013.

[16] K. Kwon, M. Seo, and S. Min, "Efficient multi-objective optimization of gear ratios and motor torque distribution for electric vehicles with two-motor and two-speed powertrain system," *Appl. Energy*, vol. 259, Feb. 2020, Art. no. 114190.

[17] C. T. P. Nguyen, B.-H. Nguyễn, J. P. F. Trovão, and M. C. Ta, "Optimal drivetrain design methodology for enhancing dynamic and energy performances of dual-motor electric vehicles," *Energy Convers. Manage.*, vol. 252, Jan. 2022, Art. no. 115054.

[18] K. Kwon, S.-K. Lim, D. Kim, and K. Park, "Automation program for optimum design of electric vehicle powertrain systems based on artificial neural network," *eTransportation*, vol. 18, Oct. 2023, Art. no. 100267.

[19] M. Zhao, J. Shi, and C. Lin, "Optimization of integrated energy management for a dual-motor coaxial coupling propulsion electric city bus," *Appl. Energy*, vol. 243, pp. 21–34, Jun. 2019.

[20] X. Yu, C. Lin, M. Zhao, J. Yi, Y. Su, and H. Liu, "Optimal energy management strategy of a novel hybrid dual-motor transmission system for electric vehicles," *Appl. Energy*, vol. 321, Sep. 2022, Art. no. 119395.

[21] X. Yu et al., "Real-time and hierarchical energy management-control framework for electric vehicles with dual-motor powertrain system," *Energy*, vol. 272, Jun. 2023, Art. no. 127112.

[22] C. T. Nguyen, P. D. Walker, and N. Zhang, "Optimization and coordinated control of gear shift and mode transition for a dual-motor electric vehicle," *Mech. Syst. Signal Process.*, vol. 158, Sep. 2021, Art. no. 107731.

[23] M. R. Ahssan, M. M. Ektesabi, and S. A. Gorji, "Electric vehicle with multi-speed transmission: A review on performances and complexities," *SAE Int. J. Altern. Powertrains*, vol. 7, no. 2, pp. 169–182, Dec. 2018.

[24] A. G. Sarigiannidis, M. E. Beniakar, and A. G. Kladas, "Fast adaptive evolutionary PM traction motor optimization based on electric vehicle drive cycle," *IEEE Trans. Veh. Technol.*, vol. 66, no. 7, pp. 5762–5774, Jul. 2017.

[25] X. Sun, Z. Shi, G. Lei, Y. Guo, and J. Zhu, "Analysis and design optimization of a permanent magnet synchronous motor for a campus patrol electric vehicle," *IEEE Trans. Veh. Technol.*, vol. 68, no. 11, pp. 10535–10544, Nov. 2019.

[26] S. Ahn, W. Song, and S. Min, "Multiobjective optimization of a traction motor in driving cycles using a coupled electromagnetic–thermal 1D simulation," *Int. J. Energy Res.*, vol. 2023, Nov. 2023, Art. no. 8854778.

[27] K. Kwon, M. Seo, and S. Min, "Multi-objective optimization of powertrain components for electric vehicles using a two-stage analysis model," *Int. J. Automot. Technol.*, vol. 21, no. 6, pp. 1495–1505, Dec. 2020.

[28] B. Zhu et al., "Gear shift schedule design for multi-speed pure electric vehicles," *Proc. Inst. Mech. Eng., D, J. Automobile Eng.*, vol. 229, no. 1, pp. 70–82, Jan. 2015.

[29] E. B. Younes, C. Changenet, J. Bruyère, E. Rigaud, and J. Perret-Liaudet, "Multi-objective optimization of gear unit design to improve efficiency and transmission error," *Mechanism Mach. Theory*, vol. 167, Jan. 2022, Art. no. 104499.

[30] M. Y. Nassar, M. L. Shaltout, and H. A. Hegazi, "Multi-objective optimum energy management strategies for parallel hybrid electric vehicles: A comparative study," *Energy Convers. Manage.*, vol. 277, Feb. 2023, Art. no. 116683.

[31] J. Wang, W. Shen, Z. Wang, M. Yao, and X. Zeng, "Multi-objective optimization of drive gears for power split device using surrogate models," *J. Mech. Sci. Technol.*, vol. 28, no. 6, pp. 2205–2214, Jun. 2014.

[32] K. Kwon, M. Seo, H. Kim, T. H. Lee, J. Lee, and S. Min, "Multi-objective optimisation of hydro-pneumatic suspension with gas–oil emulsion for heavy-duty vehicles," *Vehicle Syst. Dyn.*, vol. 58, no. 7, pp. 1146–1165, Jul. 2020.

[33] F. L. Gao, Y. C. Bai, C. Lin, and I. Y. Kim, "A time-space kriging-based sequential metamodeling approach for multi-objective crash-worthiness optimization," *Appl. Math. Model.*, vol. 69, pp. 378–404, May 2019.

[34] K. Kwon, J. Lee, and S. Min, "Motor and transmission multiobjective optimum design for tracked hybrid electric vehicles considering equivalent inertia of track system," *IEEE Trans. Transport. Electrific.*, vol. 7, no. 4, pp. 3110–3123, Dec. 2021.

[35] K.-S. Cha, D.-M. Kim, Y.-H. Jung, and M.-S. Lim, "Wound field synchronous motor with hybrid circuit for neighborhood electric vehicle traction improving fuel economy," *Appl. Energy*, vol. 263, Apr. 2020, Art. no. 114618.

[36] A. Fotouhi, D. J. Auger, K. Propp, and S. Longo, "Simulation for prediction of vehicle efficiency, performance, range and lifetime: A review of current techniques and their applicability to current and future testing standards," in *Proc. 5th IET Hybrid Electr. Vehicles Conf. (HEVC)*, Nov. 2014, pp. 1–8.

[37] S.-H. Park, J.-W. Chin, K.-S. Cha, and M.-S. Lim, "Deep transfer learning-based sizing method of permanent magnet synchronous motors considering axial leakage flux," *IEEE Trans. Magn.*, vol. 58, no. 9, pp. 1–5, Sep. 2022.

[38] M. O. Oyedeji, M. AlDhaifallah, H. Rezk, and A. A. A. Mohamed, "Computational models for forecasting electric vehicle energy demand," *Int. J. Energy Res.*, vol. 2023, pp. 1–16, Feb. 2023.

[39] K. Kwon, N. Ryu, M. Seo, S. Kim, T. H. Lee, and S. Min, "Efficient uncertainty quantification for integrated performance of complex vehicle system," *Mech. Syst. Signal Process.*, vol. 139, May 2020, Art. no. 106601.

[40] M. D. McKay, R. J. Beckman, and W. J. Conover, "A comparison of three methods for selecting values of input variables in the analysis of output from a computer code," *Technometrics*, vol. 42, no. 1, pp. 55–61, 2000.

[41] M. E. Johnson, L. M. Moore, and D. Ylvisaker, "Minimax and maximin distance designs," *J. Stat. Planning Inference*, vol. 26, no. 2, pp. 131–148, Oct. 1990.

[42] K. Deb, *Multi-Objective Optimization Using Evolutionary Algorithms*. Chichester, U.K.: Wiley, 2005.